EFFECT OF MICROCAVITY PROFILE ON THE SELECTIVE EMITTER PERFORMANCE FOR THERMOPHOTOVOLTAIC

Daizen Kirikae, Yuji Suziki, Nobuhide Kasagi, and Masaya Kobe,

Department of Mechanical Engineering, The University of Tokyo, Tokyo, Japan

Abstract: Si microcavity have been developed as a selective emitter for high-efficiency micro thermophotovoltaic (TPV) power generation system. In order to examine the effect of surface profile, two different cavities are fabricated using Bosch and non-Bosch processes. In addition, vacuum arc evaporation and electron-beam evaporation are employed to deposit metal film inside the cavities. For microcavities 1.5 µm in width, an emittance peak appears near the wavelength of 3 µm, which is close to the designed value. The peak is much higher than the emittance of large cavity, showing that the resonance of electromagnetic modes plays an important role in the modification of emittance.

Key words: Thermophotovoltaic, Selective emitter, Microcavity, Vacuum arc evaporation

1. INTRODUCTION

Lithium-ion secondary battery (LIB) is now widely used for energy sources of portable electronic devices. However, its power energy density remains insufficient for a long-term operation of those devices. Since the energy consumption of portable information and telecommunications devices is continuously increased, alternative energy source to LIB is desired.

Thermophotovoltaic (TPV) power generation system (Fig. 1) is one of the promising micro power generation systems due to its large power generation density, compatibility to various kinds of fuels, and simple configuration without moving parts. However, its energy conversion efficiency remains low because of the spectral mismatch between the radiation spectra and the band gap of photovoltaic (PV) cells. Thus, spectrum control of the thermal radiation is required for high-efficiency TPVs.

Sai *et al*. [1] developed microcavities on a single crystalline tungsten surface using fast atom beam (FAB) etching. They reported a strong emittance peak corresponding to the electromagnetic resonance mode in the cavities. However, tungsten fabrication with FAB cannot be applied to large surface area. Takagi *et al*. [2] reported that Si microcavities coated with pyrolyzed carbon could be used as a selective emitter.

In the present study, we develop metal-coated Si microcavities as a selective emitter, and examine the effects of surface profile and metal deposition methods.

2. EXPERIMENT
2.1 Fabrication Process

Figure 2 shows the process flow of the Si microcavities. Firstly, 400 nm-thick electron-beam

(EB) resist (ZEP-520A, ZEON Chemicals) is spun on at 4000 rpm, baked at 180˚C for 10 minutes, and exposed an ultra-fast EB lithography system (F5112+VD01, ADVANTEST). Then, Si microcavities are etched into the substrate with a deep reactive ion etching (DRIE) system.

Both Bosch and non-Bosch processes are used to etch the microcavities. In the Bosch process, it is relatively easy to form high-aspect-ratio cavities. However, due to its cyclic etching/passivation process, relatively large surface roughness on the sidewall (i.e., "scalloping") is inevitable. Thermal oxidation followed by BHF etching is also employed to reduce the scalloping.

Finally, after sputtering Pt on backside to prevent infrared light transmission, 100 nm-thick Ti layer is deposited with inclined physical vapor deposition both EB evaporation and vacuum arc evaporation [3]. Figure 3 shows a schematic of the coaxial arc plasma gun (ARL-300, ULVAC). By arc discharge in vacuum, cathode material is evaporated and ionized. Since the
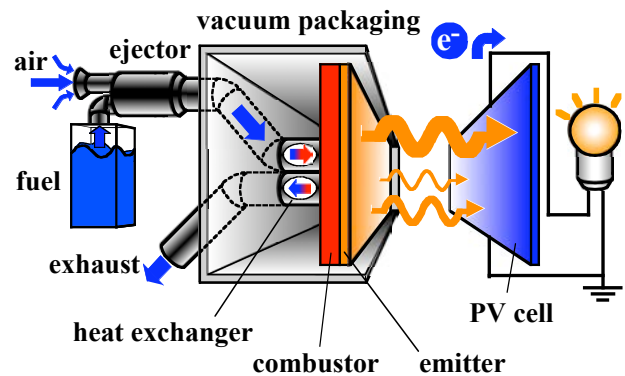

Figure 1 *TPV power generation system.*

metal particle size produced by this system is much smaller than EB evaporation and sputtering, nm-order metal films with uniform thickness can be deposited. In addition, since metal particles have higher energy than that of EB deposition, the film also has better adhesion to the Si substrate.

Kusunoki *et al.* [4] reported that the electro-magnetic resonance wavelength in the rectangular microcavity is expressed by

$$\lambda_r(n_x, n_y, n_z) = \frac{2}{\sqrt{\left(\dfrac{n_x}{L_x}\right)^2 + \left(\dfrac{n_y}{L_y}\right)^2 + \left(\dfrac{n_z}{2L_z}\right)^2}}, \quad (1)$$

where n_x, n_y = 0,1,2,3..., and n_z = 0,1,3,5.... L_x and L_y are openings of the microcavities and L_z is its depth, respectively. The maximum wavelength of λ_r corresponds to the peak emittance wavelength. In our design, the opening, the depth and the pitch are respectively 1.5 μm, 3.7 μm and 2.5 μm, corresponding to the emittance peak at the wavelength of 2.9 μm. For comparison, 8-times-larger Si cavities

1. EB lithography

2. DRIE

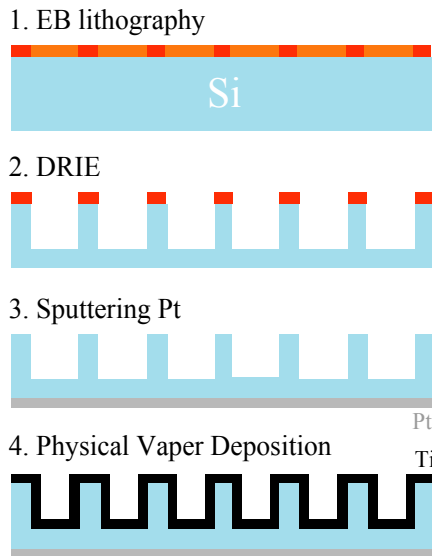3. Sputtering Pt

Pt

4. Physical Vaper Deposition

Ti

Figure 2 *Process flow of Si selective emitter.*

Trigger Electrods   Anode

Insulator

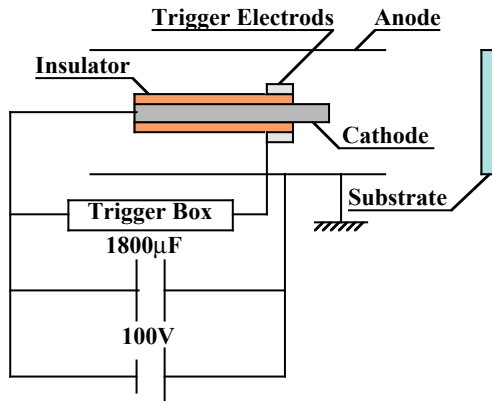Cathode

Substrate

Trigger Box
1800μF

100V

Figure 3 *Schematic diagram of arc plasma gun* [3].

with the similarity shape are also fabricated.

2.2 Experimental Setup

Figure 4 shows the experimental setup for the emittance spectrum measurements, which consists of a vacuum chamber, an infrared heat lamp (GVL2998, Thermo Riko), a graphite sample holder, an infrared spectrometer (MC-10N3G, Ritsu Applied Optics), and a radiation thermometer (KT 15.02, Heitronics). The sample is glued onto the graphite holder, and placed in the vacuum chamber with a sapphire window to prevent heat loss and oxidization, and heated up to about 900˚C at 3×10^{-3} Pa with the infrared heat lamp from the bottom. Thermal radiation from the sample is introduced to the spectrometer using two silver-coated mirrors. A lock-in amplifier (SR510, Stanford Research Systems) is employed to measure the output voltage of the spectrometer.

Emittance of the sample (ε_{sam}) is calculated using the radiation energy of the sample (E_{sam}) and that of a reference material (E_{ref}) with known emittance (ε_{ref}). In the present study, blackbody paint (JSC-3, Japan Sensor), of which emittance is 0.94, is used. Emittance of the sample is given by

$$\varepsilon_{sam}(\lambda) = \varepsilon_{ref}(\lambda) \frac{E_{sam}(\lambda)}{E_{ref}(\lambda)} \frac{\exp\left(\dfrac{hc}{kT_{sam}\lambda}\right) - 1}{\exp\left(\dfrac{hc}{kT_{ref}\lambda}\right) - 1}, \quad (2)$$

where h, c, k, λ and T are respectively Planck's constant, the light speed, Boltzmann constant, the wavelength and the sample temperature measured with the radiation thermometer.

Uncertainty interval of the emittance can be expressed by

$$\frac{d\varepsilon_{sam}(\lambda)}{\varepsilon_{sam}(\lambda)} \approx \left[\left| \frac{dE_{sam}(\lambda)}{E_{sam}(\lambda)} \right|^2 + \left| \frac{dE_{ref}(\lambda)}{E_{ref}(\lambda)} \right|^2 \right.$$

$$\left. + \left| \frac{hc}{kT_{sam}\lambda} \frac{dT_{sam}}{T_{sam}} \right|^2 + \left| \frac{hc}{kT_{sam}\lambda} \frac{dT_{ref}}{T_{ref}} \right|^2 \right]^{\frac{1}{2}}, \quad (3)$$

where error in the emittance of the reference material is assumed to be negligible.

At λ = 1μm, where uncertainty becomes maximum, the estimate of uncertainty interval at the 95% coverage is within 10% for $T_{sam} = T_{ref}$ = 900˚C. Major source of the uncertainty is the sample temperature measurement.

3. RESULTS
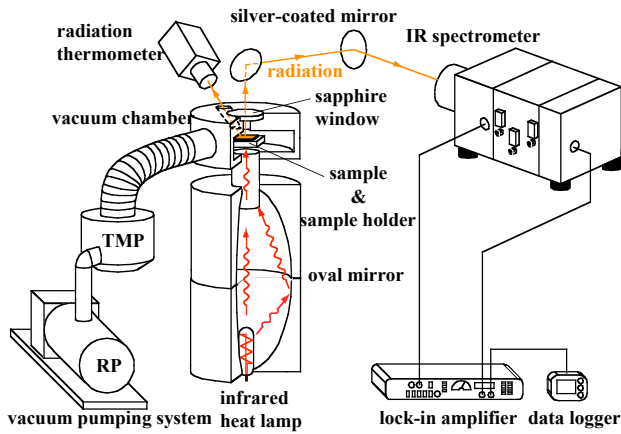### 3.1 Cavity Profile with Different Fabrication Methods
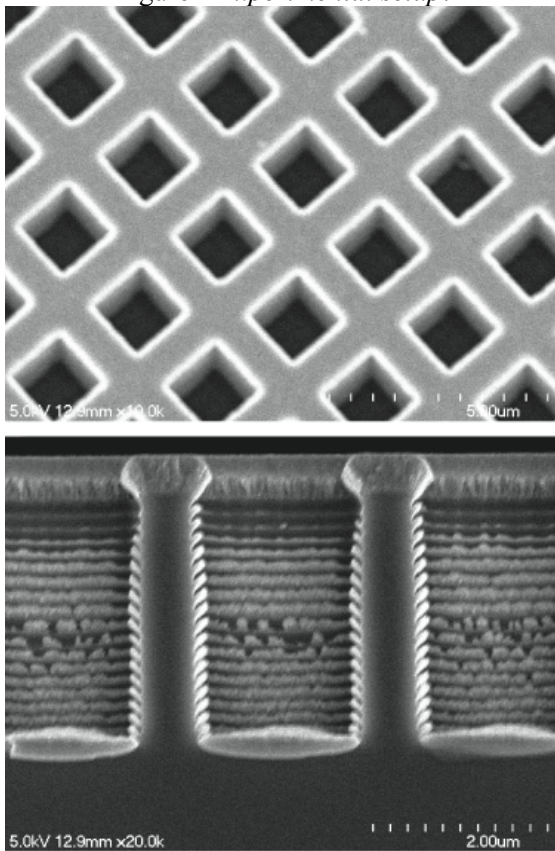
Figure 4 *Experimental setup*.

Figure 6 *Si microcavities fabricated with non-Bosch DRIE process and inclined EB deposition of Ni.*

Figure 5 *Si microcavities fabricated with Bosch DRIE process and inclined EB deposition of Ti*

Figure 7 *Si microcavities fabricated with non-Bosch DRIE process and inclined deposition of Ni using vacuum arc evaporation*.

Figure 5 shows SEM images of the Ti-coated Si microcavities with the Bosch process and the EB evaporation. Arrays of microcavities with vertical walls are successfully developed. However, the scalloping is clearly seen on the sidewall, because the metal layer becomes discontinuous.

Figure 6 shows SEM images of Ni-coated Si microcavities fabricated with non-Bosch DRIE process. Roughness on the sidewall is significantly reduced if compared with the microcavities with the Bosch process. However, the metal layer surface is somewhat rough, as shown in Fig. 8. The dimensions of the roughness elements are on the order of 100 nm. On the
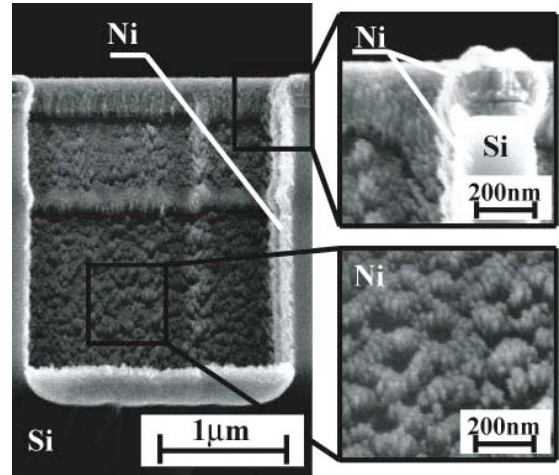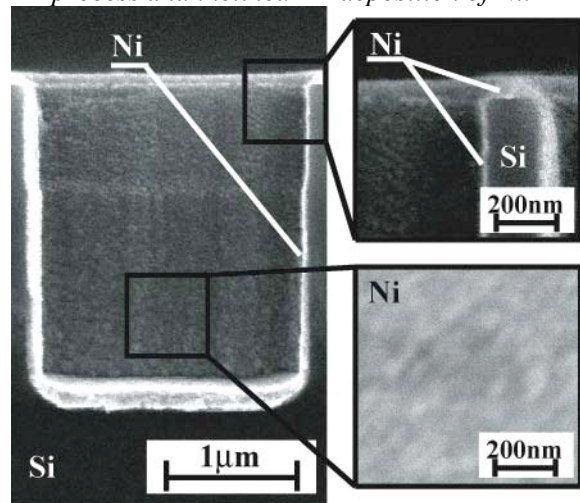
other hand, when the vacuum arc evaporation is employed, the metal surface becomes much smoother as shown in Fig. 7.

3.2 Emittance Spectra Measurement

Firstly, in order to validate the present measurement, the radiation energy of the substrate coated with blackbody paint was measured twice, and the emittance obtained is compared with the reference value. Figure 8 shows the experimental results. Although the emittance is slightly increased with the wavelength, the reference value of 0.94 is within the uncertainty interval at almost all the wavelengths.

Figure 9 shows the emittance spectra of microcavities obtained at about 900°C. The emittance exhibits a marked peak at 3 μm, which is close to the designed value of 2.9 μm. The effect of surface roughness is also clearly seen; when the surface roughness is reduced by thermal oxidation and BHF-etching, the emittance peak becomes larger. It is
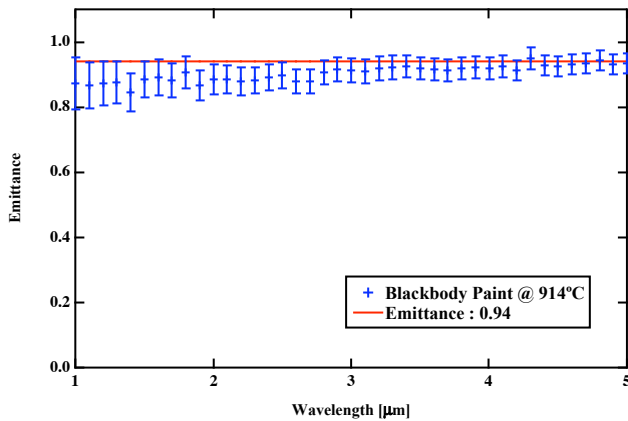
Figure 8 *Experimental results for the emittance of the reference material at about 900°C.*
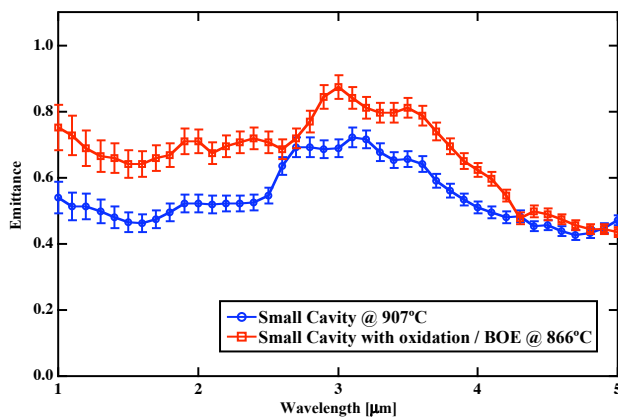

Figure 9 *Effect of surface roughness on the emittance spectra. Si microcavities are fabricated with the Bosch process and the EB evaporation. Sample temperature is at about 900°C.*
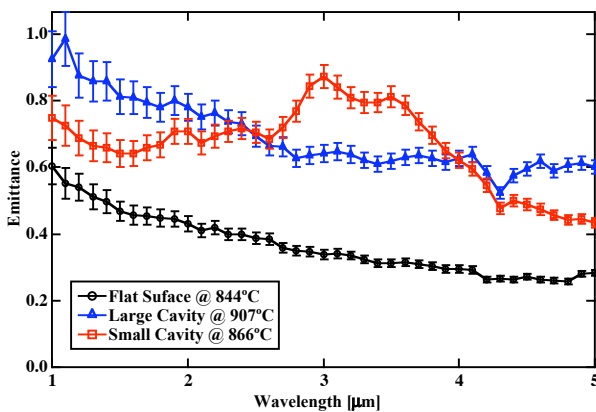

Figure 10 *Emittance spectra of the Si microcavities fabricated with the Bosch process and the EB evaporation. Sample temperature is at about 900°C.*

conjectured that microcavities with non-Bosch process and the vacuum arc evaporation (Fig. 7) should have better performance.

Figure 10 shows the emittance of microcavities in comparison with those of the flat surface and the large cavities. The emittance of the large cavities is higher than that of the flat surface, showing the effect of surface area increase. Emittance for both case is monotonically decreased with increasing wavelength, and respectively 0.64 and 0.34 at 3 μm. On the other hand, the emittance of the small cavities exhibits a marked peak at 3 μm, and its peak value is as large as 0.87, showing the electromagnetic resonance. Thus, it is confirmed that not only the effect of surface area increase but also the effect of electromagnetic resonance plays a dominant role.

When InGaAsSb PV cell, of which bandgap wavelength is 2.3 mm is assumed, ideal energy conversion efficiency is estimated to be 19% for blackbody at 900 °C. When the present microcavities are employed with appropriate cavity dimensions, the estimate of the efficiency is much improved to 29%.

4. CONCLUSION

The effect of surface profile on the radiation spectra of microcavities is investigated to develop selective emitter for TPVs. Different fabrication methods for the microcavity etching and the metal film deposition are examined. We found that the surface roughness has a large effect on the electromagnetic resonance modes in the microcavities. We have also demonstrated that metal-coated Si microcavities exhibit a strong emittance peak at the wavelength of 3 μm, which is in good agreement with its designed value.

REFERENCES

[1] Sai, H., Kanamori, Y., and Yugami, H., "High-temperature resistive surface grating for control of thermal radiation," *Appl. Phys. Lett*., **82**, (2003) 1685-1687.

[2] Takagi, D., Suzuki, Y., and Kasagi, N., "Pyrolyzed parylene structure as selective emitter for high-efficiency thermophotovoltaic power generation," *Proc. IEEE Int. Conf. MEMS2007*, Kobe, (2007) 883-886.

[3] Yamamoto, Y., Agawa, Y., Hara, Y., Amano, S., Chayahara, A., Horino, Y., and Fujii, K., "Development of a coaxial type vacuum arc evaporation source", *Proc. IEEE Int. Conf. Ion Implantation Technology*, Kyoto, (1998) 1148-1150.

[4] Kusunoki, F., Takahara, J., and Kobayashi, T., "Quantitative change of resonant peaks in thermal emission from periodic array of microcavities", *Electronics Lett*, **39**, (2003) 23-24.